Journal of the European Ceramic Society 19 (1999) 1717–1724

PII: S0955-2219(98)00267-2
0955-2219/99/$ - see front matter

Colloidal Stability and Sintering of Yttria–Silica and Yttria–Silica–Alumina Aqueous Suspensions

M. Aparicio,* R. Moreno and A. Durán

Instituto de Cerámica y Vidrio (CSIC), E-28500 Arganda del Rey, Madrid, Spain

(Received 17 September 1998; accepted 25 October 1998)

Abstract

The aim of this work was to produce dense yttrium silicate materials by slip casting, with more than 90% of Y_2SiO_5 phase. The rheological behaviour of concentrated aqueous slips was studied considering the effect of the dispersing additives, solids content and pH. The densification kinetics was examined as a function of temperature and time, and the reactions were analysed in the light of the equilibrium phase diagrams. Deflocculation of the slips was achieved by either an electrostatic mechanism using tetraethylammonium hydroxide, thus requiring a high concentration of base, and by a polyelectrolyte through an electrosteric mechanism, which provided more reliable results. In the binary system Y_2O_3–SiO_2, a very low grade of sintering was obtained at 1600°C. The use of alumina allows sintering through a liquid phase, reaching 90% theoretical density.

Keywords: slip casting, suspensions, yttrium silicate, silicate, sintering.

1 Introduction

The development of aero-engine and aircraft is close related to ceramic matrix composites (CMC) and intermetallics, specially fibre reinforced ceramics based in C/SiC.[1,2] However, these materials can only be used without protection up to 450°C, due to the susceptibility to oxidation of the carbon fibre and the most usual method employed for their protection is the deposition of external coatings. In general, all multilayer systems use SiC as internal coating for their evident likeness with the substrate.[3,4]

Different compositions have been studied to complement SiC coatings. One interesting material seems to be yttrium silicate (Y_2SiO_5), obtained by Ogura *et al.*[5] by hot isostatic pressure at 1700°C with Y_2O_3 as secondary phase. The resulting material combines a low Young modulus with a small thermal expansion coefficient, very close to that of SiC. These properties ensure high stability for the multilayer and very small residual stresses in the interface SiC/Y_2SiO_5. Their low evaporation rate and oxygen permeability complete an excellent group of antioxidant characteristics.[6]

Processing is always a key step in the development of any material or device. The use of concentrated colloidal suspensions allows to reach thick coatings as a function of the substrate porosity. The optimization of colloidal suspensions in order to reach a low viscosity, high zeta potential and high density is the first step in order to produce homogeneous, defect free pieces or coatings.[7] The problem gains complexity when colloidal suspensions are formed by two or more types of particles because each type of particle interacts with the others. The colloidal properties of yttria/silica aqueous suspensions have been studied by authors that discuss the possible dissolution of species promoting coagulation of such heterogeneous mixtures.[8,9] The following stage in the process is the design of the thermal treatment that leads to the required phases and an adequate densification. The main factors that control sintering are temperature, time and furnace atmosphere. An important aid for the correct design of the heat treatment is the previous study of the equilibrium phase diagrams of involved phases, that allow to know the percentage of each phase appearing at each temperature in equilibrium conditions. Additives permit, in some cases, to enhance the sintering process through the formation of transient liquid phases. The effect of these additives on the final composition can also be studied through equilibrium phases diagrams.

The aim of this work was to develop a feasible procedure to produce dense bulk yttrium silicate

*To whom correspondence should be addressed.

materials for further application as protective coating onto SiC substrates. For this reason, the suspension should have an adequate viscosity and stability for the coating process, and the sintering should be developed to fulfil determined conditions:

1. High densities.
2. Maximum sintering temperature of 1600°C, since this temperature is critical for the stability of C/SiC substrate.
3. Final compositions with more than 90% of Y_2SiO_5 phase.

2 Experimental

2.1 Starting powders

The following commercial powders were used as starting materials: (1) Y_2O_3 (Mandoval, UK), with a mean particle size of 3·5 μm, a specific surface area of 6·9 $m^2 g^{-1}$, a density of 5·83 $g cm^{-3}$ and a purity higher than 99·9%; (2) a microcrystalline SiO_2 (Sigma, USA) with a mean particle size of 2·5 μm, a specific surface area of 5·5 $m^{2-1}g$ and a purity of 99%. An Al_2O_3 (Condea HPA05, Germany) with a mean particle size of 0·5 μm, a specific surface area of 9·5 $m^2 g^{-1}$, a density of 3·98 $g cm^{-3}$ and a purity higher than 99·9% was used as sintering additive to improve densification by means of a transient liquid phase.

2.2 Selection of compositions

Y_2O_3:SiO_2 mixtures with relative mole contents of 50:50 and 51:49 were prepared. These binary compositions were labelled B1 and B2, respectively. These mixtures were selected taking into account the equilibrium phase diagram of the binary system Y_2O_3–SiO_2 (Fig. 1), that shows that the equimolar ratio should allow to obtain the maximum percentage of the metasilicate phase.[10] Compositions with some Y_2O_3 in excess give place to a mixture of metasilicate and pure Y_2O_3 with an invariant point at 1800°C. On the other hand, an excess of silica should promote the formation of yttrium disilicate ($Y_2Si_2O_7$) and an eutectic point appears at much lower temperature (1660°C).

Mixtures including Al_2O_3 as sintering aid were also considered. Compositions of Y_2O_3:SiO_2:Al_2O_3 in relative mole contents of 50·5:48·5:1·0, 48:49:3 and 48·75:49·75:1·5 were selected because they are located in different compatibility regions in the ternary phase diagram which present different invariant points. They were labelled as T1, T2 and T3, respectively. Figure 2 shows the Y_2O_3–SiO_2–Al_2O_3 equilibrium phase diagram, including the compatibility triangles.[10] The phase Y_2SiO_5 constitutes the corner of four compatibility triangles. The first considered composition (point T1) was selected to obtain Y_2SiO_5 with a densification higher than that obtained from the 49:51 binary mixture. The diagram shows that compositions located inside the compatibility triangles I, II and III do not reach the liquidus surface at 1600°C, only solid phases appearing at this temperature. However, the invariant point corresponding to triangle IV is around 1530°C, and the phases appearing at 1600°C should be YS + Y_3Al_5 + L (Fig. 3). Thus, composition T2 (Fig. 3) was selected considering the following calculated percentages of phases at 1600°C: 89·4% YS, 2·3% Y_3Al_5 and 8·3% liquid. This liquid should enhance the sintering at 1600°C. The cooling of this composition in equilibrium conditions should produce about 82% Y_2SiO_5 and 18% of phases $2Y_2O_3{\cdot}3SiO_2 + 3Y_2O_3{\cdot}5Al_2O_3$. From the binary diagram Y_2O_3–SiO_2 it is observed that phase $2Y_2O_3{\cdot}3SiO_2$ is stable at high temperature, giving $Y_2O_3{\cdot}SiO_2 + Y_2O_3{\cdot}2SiO_2$ at room temperature. Thus, the final percentage of $Y_2O_3{\cdot}SiO_2$

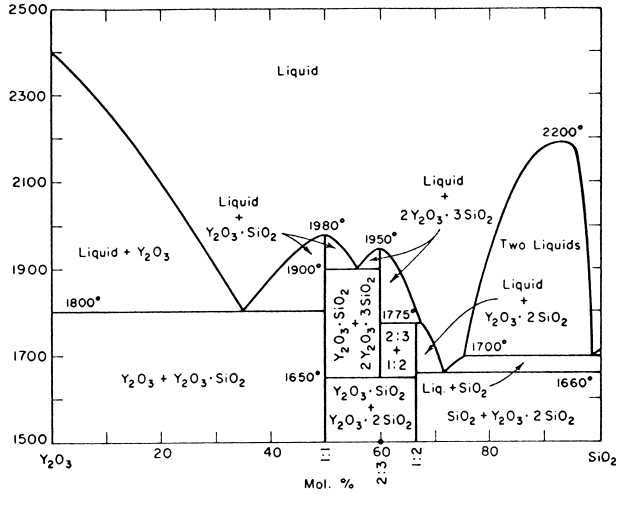

Fig. 1. Y_2O_3–SiO_2 phase equilibrium diagram.[10]

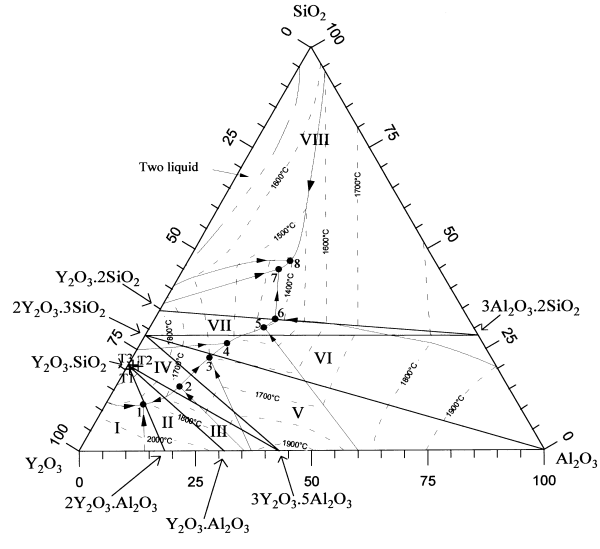

Fig. 2. Y_2O_3–SiO_2–Al_2O_3 phase equilibrium diagram.[10]

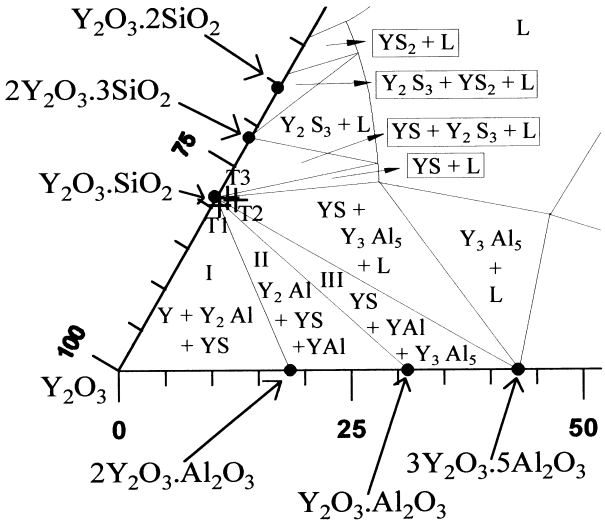

Fig. 3. Isothermal section at 1600°C of Y_2O_3–SiO_2–Al_2O_3 system.

should be around 86% with around 5% of $Y_2O_3{\cdot}2SiO_2$ and 9% of $3Y_2O_3{\cdot}5Al_2O_3$. The third ternary composition (T3), is located between the point T2 and that corresponding to the pure Y_2SiO_5 phase (Fig. 2), also in the compatibility triangle IV. The aim of this composition was to obtain higher percentage of Y_2SiO_5 without surpassing 1600°C, and to analyse the influence of the additive reduction on the final density, since reducing the percentage in Al_2O_3 the quantity of liquid phase at high temperature diminishes (about 4% at 1600°C).

2.3 Preparation of the slips

All the studied compositions were prepared by colloidal filtration from aqueous concentrated slips. The slips were prepared using a ball mill with Al_2O_3 balls and jar for 4 h. The rotary mill causes the agglomerated particles to redisperse, thus decreasing the mean particle size and increasing the surface area.

The isoelectric point (iep) of SiO_2 was not measured because it has been profusely reported and occurs at acidic pHs, usually at values of 2–4. The isoelectric point of Y_2O_3 was reported to occur at pH 8.5 in a previous work.[11] However, in that work it was observed that after milling, the isoelectric point shifts up to pH 9 and the absolute values of zeta potential are lower at any pH. From the isoelectric points, basic conditions should be preferred for the preparation of stable concentrated slips. Thus, an alkali-free strong base, tetraethylammonium hydroxide (TMAH), have been used as dispersant to achieve the slip stabilization by a pure electrostatic mechanism. Moreover, a carbonic acid based polyelectrolyte (Dolapix CE-64, Zshimmer-Schwarz, Germany) was also used to provide stabilisation by means of an electrosteric mechanism.

Viscosity measurements were performed using a rotational viscosimeter with a coaxial cylinders system (Haake, Rotovisco RV20, Germany), at a constant temperature of 25°C. Two different cycles were used for rheological determination.The first was used to determine the flow curve, in which the shear rate was increased from zero to maximum velocity (2700 s^{-1}) in 2 min, 1 min at that speed and back to zero in 2 min. A second cycle was used to observe the time dependence, consisting in a similar cycle but maintaining the maximum speed for 10 min.

Once the slip preparation procedure was optimized, slips of the different compositions were slip cast onto plaster of Paris moulds to obtain disks with 2 cm in diameter. The cast specimens were left in air for 48 h to dry before sintering experiments. The thermal treatments were performed in an electric furnace in air.

The final density of sintered compacts was measured by Hg immersion method. The study of the phases was made in the light of the equilibrium phase diagrams by XRD (Siemens, model D5000). Microstructural observations were performed with a scanning electron microscopy (Zeiss, model DSM-950) on polished and thermal etched surfaces. Phase analysis was carried out by energy-dispersive microanalysis (EDX).

3 Results and Discussion

3.1 Slip behaviour

Initially, the equimolar binary composition (B1) was prepared using TMAH as deflocculant. To ensure a proper mixing of concentrated slips, the initial pH of the mixture must be away from the isoelectric point. So, for solid loadings as high as 65 wt%, the preparation of slips is only possible if the starting pH is $\geqslant$11. When the initial pH prior to mixing is lower than the iep, the mixture strongly agglomerates and further additions of TMAH do not redisperse the highly viscous slips. This is likely produced by an heteroflocculation mechanism because yttria and silica particles are oppositely charged, thus promoting the adsorption of yttrium ions onto silica surface. Slips at solid loadings of 65 wt% can be prepared by adjustments of pH to values higher than.[11] Fig. 4 presents the flow curves of the slip with 65 wt% solid content at pH of 11·8 and 12·6. At the first pH, the obtained viscosity is too high (60 mPa s at a shear rate of 2700 s^{-1}) and the slip shows a complex rheological behaviour corresponding to a thixotropic thickener, where both the up and the down curves behave as dilatant, but at the maximum speed particles rearrange thus decreasing the viscosity.

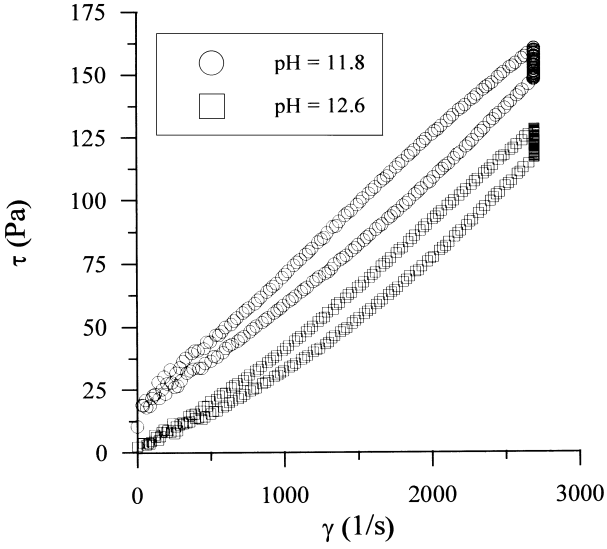

Fig. 4. Flow curves of 65 wt% solid $50Y_2O_3$:$50SiO_2$ slips at different pH.

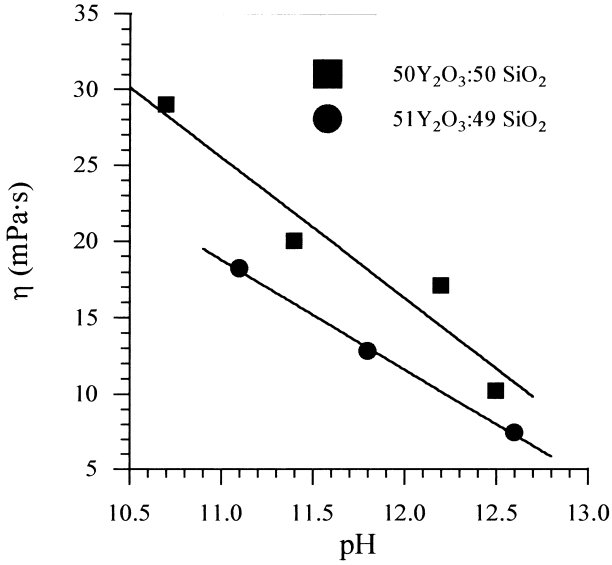

Fig. 5. Variation of viscosity with pH at 500 s^{-1} of 60 wt% solid $50Y_2O_3$:$50SiO_2$ and $51Y_2O_3$:$49SiO_2$ slips.

On the other hand there is a significant yield value (~15 Pa) corresponding to a plastic fluid. A small increase in pH up to 12·6 does not modify the curve habit, but reduces the viscosity (48 mPa s at a shear rate of 2700 s^{-1}), the yield value practically disappears and the time dependency after 10 min is reduced to a half. However, a big amount of base is required to achieve this pH, which seriously limits the castability of the slip.

These problems led to the preparation of slips with lower solid contents, such as 60 wt%, which can be easier prepared, although pHs higher than 11 are also required for a complete dispersion. The viscosity corresponding to pH 12·5 B1 slip decreases now to 27 mPa s at a shear rate of 2700 s^{-1}. For B2 composition, the viscosity is slightly lower (21 mPa s at a shear rate of 2700 s^{-1} at pH 12·6). In both cases there is no yield value. Figures 5 and 6 plot the variation of viscosity of both slips with pH for 500 and 1000 s^{-1}. When pH increases the viscosity is always reduced, as a consequence of the increased stability reached at longer separations from the iep of yttria. According to this rheological behaviour, slips containing 60 wt% of solids were selected for casting experiments.

Anyway, the effect of TMAH as pH-adjuster is not enough to completely stabilize these slips. To improve the dispersability a polyelectrolyte was tested, so that electrosteric stabilization is promoted. In this stabilizing mechanism there is not a primary minimum in the potential energy curve and, consequently, there is not a direct contact between particles and coagulation is prevented. Nevertheless, the existence of a secondary minimum makes possible the weak flocculation of particles, but the so formed flock can be easily redispersed.

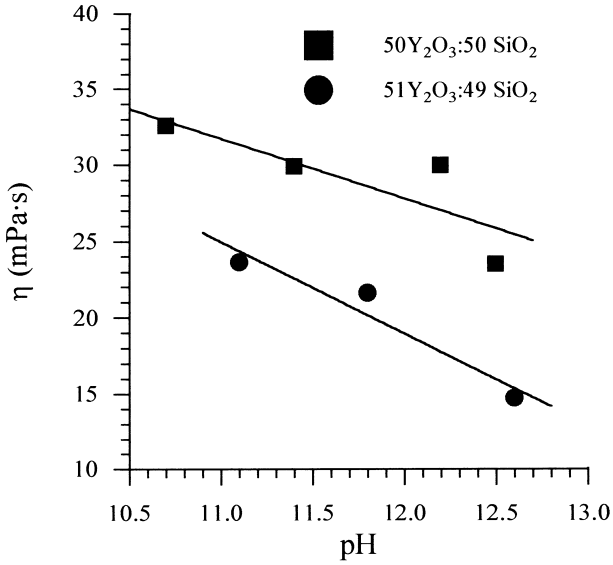

Fig. 6. Variation of viscosity with pH at 1000 s^{-1} of 60 wt% solid $50Y_2O_3$:$50SiO_2$ and $51Y_2O_3$:$49SiO_2$ slips.

The rheological behaviour of the slips was studied as a function of the concentration of deflocculant. Figure 7 shows the flow curves of B2 slips prepared with different deflocculant concentrations. The regression of these curves give Newtonian model as best fit, although for slips containing 1 wt% deflocculant, a slightly dilatant behaviour is clearly observed in the plot. Lower viscosities are obtained for increasing deflocculant concentrations, although for 1·5 wt% a small yield value is detected. Slips with 2 wt% deflocculant have no yield value. The viscosity after fitting according to Newton are 10·4, 9·5 and 9·3 mPa s, respectively, and hence slips were furtherly prepared with 2 wt% Dolapix. Figure 8 shows the flow curves of B1 and B2 compositions dispersed with 2 wt% deflocculant and a total solid loading of

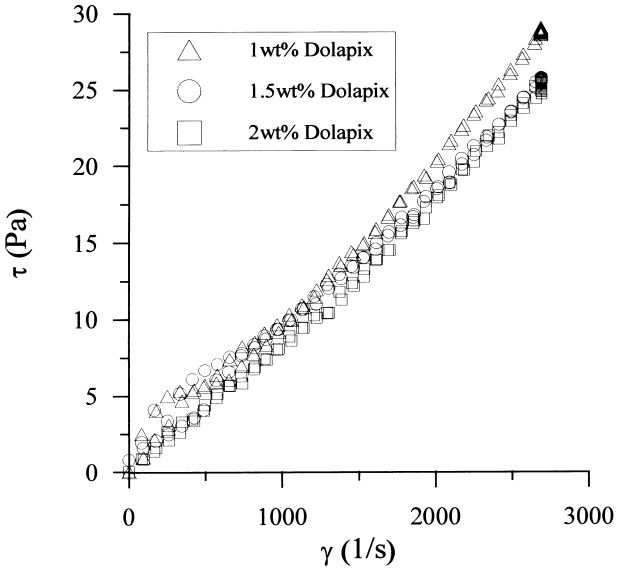

Fig. 7. Flow curves of 60 wt% solid $51Y_2O_3$:$49SiO_2$ slips with 1, 1·5 and 2 wt% Dolapix CE-64 as dispersant.

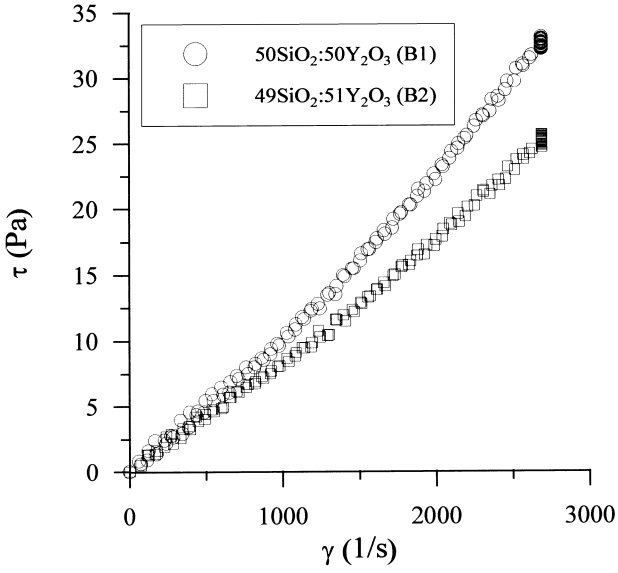

Fig. 8. Flow curves of 60 wt% solid Y_2O_3:SiO_2 slips with 2 wt% Dolapix CE-64 as dispersant.

60 wt%. At these dispersing conditions, the rheological behaviour of the slips can be fitted also to a Newtonian model, but the viscosity values slightly decrease when there is Y_2O_3 in excess, similarly to the behaviour observed when TMAH is used as pH-adjuster. The resulting viscosity for these slips is around 10 mPas, lower than those obtained for the slips dispersed with TMAH. This provides an improved route for the preparation of low viscosity, castable slips, that was used for subsequent experiments.

These conditions were also selected for the preparation of slips containing Al_2O_3 as sintering aid. The resulting rheological behaviour is practically the same to that of the binary mixtures, the additive does not modify the rheology, which is also Newtonian, and presents a viscosity lower than 10 mPa s. This can be explained by the low concentration (a maximum of 3 mole%) of alumina, that presents a similar iep to that of yttria.

Green samples of binary and ternary compositions were obtained by casting on plaster molds 60 wt% slips dispersed with 2 wt% polyelectrolyte. The relative density of dry casts were in all cases between 47 and 50% theoretical.

3.2 Densification and phase analysis

As a first approach the densification of the equimolar binary system (B1) was followed by static sintering at different temperatures and times. Figure 9 depicts the final density as a function of temperature for 3 h of sintering. As shown, density values increase linearly with temperature, thus suggesting that the same mechanism is operating. Since Y_2SiO_5 phase is the only phase appearing for the four temperatures, following the phase diagram (Fig. 1), this indicates that sintering is occurring by solid state diffusion, being activated only by temperature. However, the relative densities are quite low, reaching a value of only 73% at 1670°C (Y_2SiO_5 crystallographic density, 4·4 g cm^{-3}). In Fig. 10 the XRD spectra corresponding to each point of Fig. 9 are shown. At 1500°C the major phase is Y_2SiO_5, but a significant amount of Y_2O_3 remains still unreacted, since the following reaction has not been completed:

$$SiO_2 + Y_2O_3 \rightleftharpoons Y_2SiO_5 \qquad (1)$$

As a consequence, the remaining free silica reacts with part of the Y_2SiO_5, originating a small fraction of $Y_2Si_2O_7$ (crystallographic density, 4·1 g cm^{-3}):

$$SiO_2 + Y_2SiO_5 \rightleftharpoons Y_2Si_2O_7 \qquad (2)$$

When temperature increases up to 1550 and 1600°C, equilibrium in eqn (1) displaces to the formation of Y_2SiO_5 and the relative concentrations of Y_2O_3 and $Y_2Si_2O_7$ continuously decrease. At 1670°C, the major phase is still Y_2SiO_5, but a new secondary phase appears containing $Y_{4.67}(SiO_4)_3O$ together with $Y_2Si_2O_7$. The existence of this phase was reported by Ogura,[5] although this phase disappears at 1900°C after 10 h treatment, decomposing in Y_2SiO_5 and SiO_2. This complex phase has a stoichiometry close to the phase $2Y_2O_3{\cdot}3SiO_2$, which, according to the phase diagram (Fig. 1), appears at temperatures higher than 1650°C.

According to these consideration, a thermal treatment of 1600°C was fixed for further experiments because this is the limit for applications onto SiC substrates, and provides the higher relative

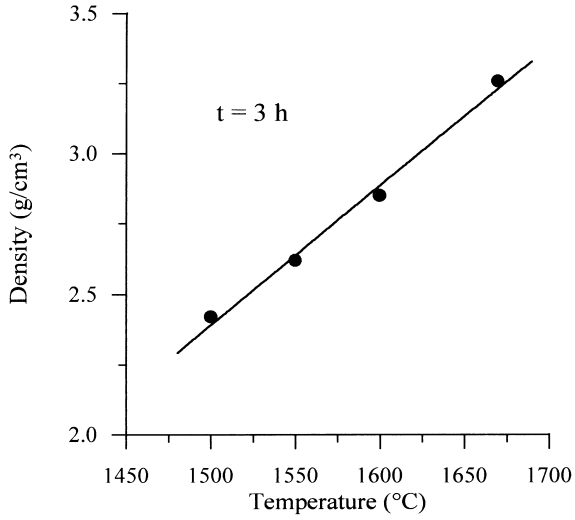

Fig. 9. Density of $50Y_2O_3$:$50SiO_2$ at different temperatures (3 h).

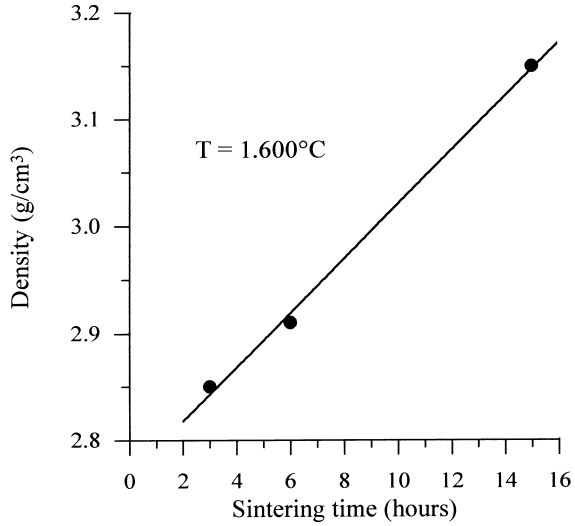

Fig. 11. Density of $50SiO_2$:$50Y_2O_3$ at different times at 1600°C.

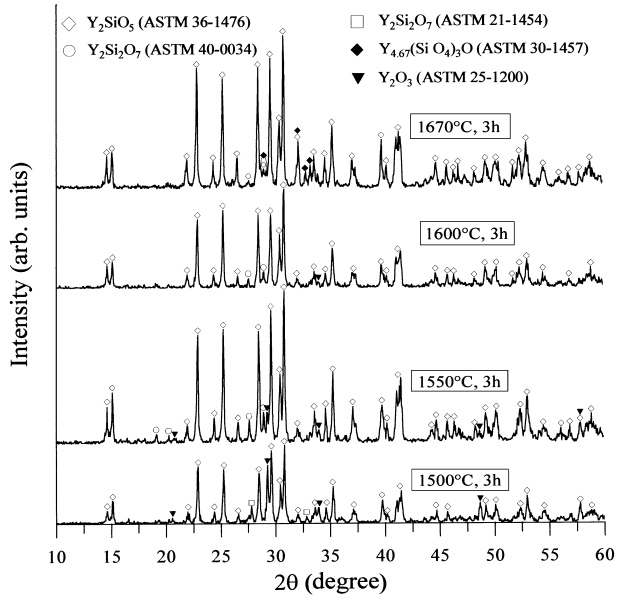

Fig. 10. XRD patterns of $50Y_2O_3$:$50SiO_2$ at different temperatures (3 h).

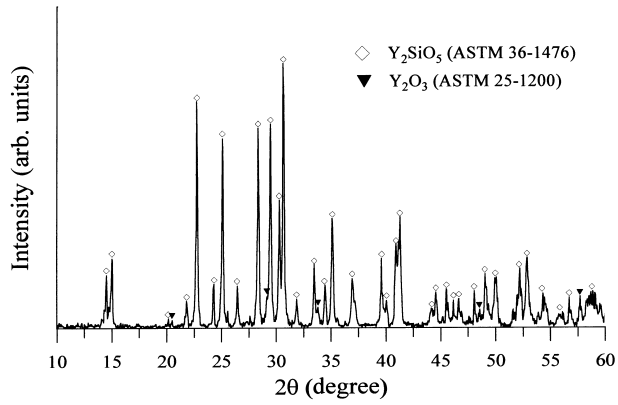

Fig. 12. XRD pattern of $51Y_2O_3$:$49SiO_2$ at 1600°C (3 h).

content of Y_2SiO_5. However, the final density is rather low. For this reason, the evolution of density as a function of sintering time has been also studied at this temperature (Fig. 11). The relative densities increase from 64% for sintering times of 3 h to 71% after 15 h at 1600°C. XRD patterns demonstrate that the only effect of increasing sintering time is to obtain better crystallized samples, but no different phases appear.

In the case of the non-equimolar binary mixture (B2), after a heat treatment at 1600°C for 3 h final densities did not surpass a density of 54% theoretical. On the other hand, the XRD patterns show that the small increase in Y_2O_3 content avoids the appearance of $Y_2Si_2O_7$, (Fig. 12). The low sintering degree is probably caused by the shifting of the composition to the left side of the phase equilibrium diagram, where the formation of the $Y_2Si_2O_7$ phase does not occur. This phase is associated with a lower invariant point (1660°C) that facilitates sintering by solid state diffusion.

Sintering studies were also performed for compositions including Al_2O_3 as sintering aid. The first considered composition (point T1 in Fig. 2) corresponds to the molar composition $50{\cdot}5Y_2O_3$: $48{\cdot}5SiO_2$:$1.0Al_2O_3$. After 3 h at 1600°C the density remains very low (2·64 g cm^{-3}, 59% th.). The isothermal section at 1600°C (Fig. 3) shows that this composition has not reached the liquidus surface, located between stability fields I and II, whose invariant points are 1800 and 1675°C (points **1** and **2** in the same figure), higher than sintering temperature. The second selected composition (T2 in Fig. 2) was $48Y_2O_3$:$49SiO_2$:$3Al_2O_3$, and the presence of liquid phase should act enhancing densification at 1600°C. A heat treatment of this composition at 1600°C for 3 h produced a final density of 4·0 g cm^{-3} (90% of th.), confirming the previous hypothesis. The microphotograph (Fig. 13) allows to distinguish the presence of the three phases: the matrix (A) that correspond, according to EDX, to the phase $Y_2O_3{\cdot}SiO_2$; the

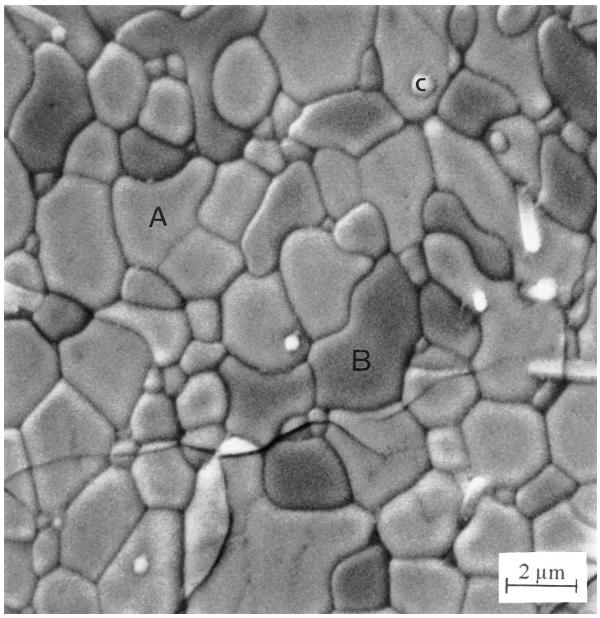

Fig. 13. SEM microphotograph of $48Y_2O_3$:$49SiO_2$:$3Al_2O_3$ sintered at 1600°C (3 h).

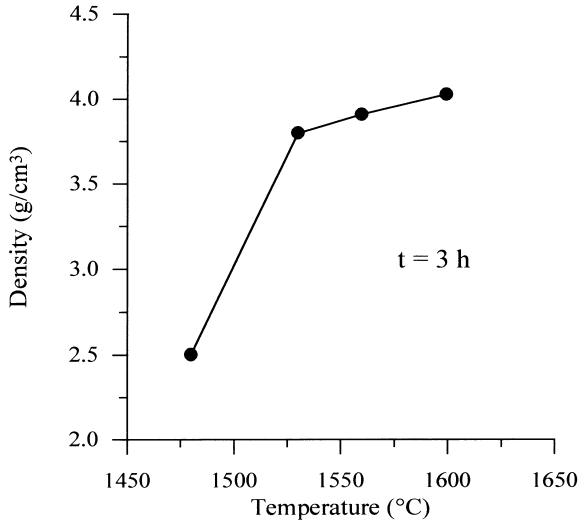

Fig. 14. Density of $48Y_2O_3$:$49SiO_2$:$3Al_2O_3$ at different temperatures (3 h).

second phase in quantity and with a darker tone (B), corresponds to $3Y_2O_3{\cdot}5Al_2O_3$; and the third phase, that appears as small and very clear spheres (C), seems to be $Y_2O_3{\cdot}2SiO_2$, although due to their small diameter (below 1 μm), they could not be identified by EDX. These results confirm the predictions derived from the equilibrium phases diagram, indicating that the material is close to the thermodynamic equilibrium.

These results allowed to decrease the sintering temperature, an important goal in the future coating process. Figure 14 is a plot of density as a function of temperature, for a constant sintering time of 3 h, and shows an important increase at 1530°C, the temperature corresponding to the invariant point of region IV. Figure 15 presents the

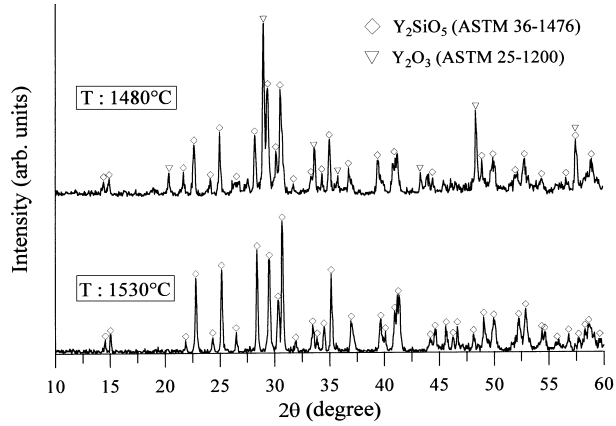

Fig. 15. XRD patterns of $48Y_2O_3$:$49SiO_2$:$3Al_2O_3$ at different temperatures (3 h).

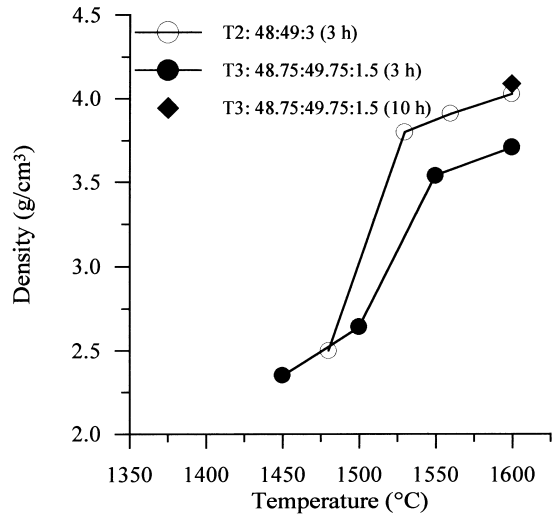

Fig. 16. Density of $48Y_2O_3$:$49SiO_2$:$3Al_2O_3$ and $48{\cdot}75Y_2O_3$:$49{\cdot}75SiO_2$:$1{\cdot}5Al_2O_3$ at different temperatures and times.

XRD patterns corresponding to each point of Fig. 14. The phase appearing at 1530°C is the same observed at 1560 and 1600°C (Y_2SiO_5), but it changes when temperature is further lowered. The pattern corresponding to 1480°C shows Y_2O_3 as main phase; although an important percentage of Y_2SiO_5 has been already formed, the pattern denotes that the raw materials has not completely reacted.

Upon comparing the density of the last ternary composition (T3) with temperature for treatments of 3 h (Fig. 16), a lower sintering level is observed. For 1600°C, the reached density was 84% against 90% reached by composition T2. A treatment of 10 h at 1600°C allows to reach a density slightly higher to that of composition T2 at the same temperature with only 3 h of treatment. This behaviour results from the decrease of the percentage of liquid phase that reduces sintering rate, although the same final densities are reached in both cases. XRD show a similar behaviour to that observed in composition T2.

4 Conclusions

Binary Y_2O_3:SiO_2 colloidal suspensions with very low viscosity have been prepared with a solid content of 60 wt%. Electrostatic stabilization by means of TMAH requires big concentrations of the base, which difficults slips preparation and provides viscosity values adequate for slip casting, but too high for the coating applications sought in this work.

Improved slip behaviour was obtained by electrosteric stabilization using a polyelectrolyte, giving viscosities of 10 mPa s, low enough for dipping. The addition of low concentration of a third component (Al_2O_3, as sintering aid) does not practically modify the rheological behaviour and hence, uniform, stable slips can be also prepared.

Sintering of binary system Y_2O_3:SiO_2 at 1600°C prevents the formation of a liquid phase lowering the densification, and leading to final densities less than 65% theoretical, through a solid state sintering mechanism.

Al_2O_3 is a good additive that allows to get 90% theoretical density, since sintering takes place through a liquid phase.

Acknowledgements

This work have been partially financed by Brite Euram Programme BRE-CT94-0907 (Project No. BE-93-7059) in collaboration with Daimler-Benz Aerospace (Germany), Sintec CVD (UK), and UMIST (University of Manchester). The cooperation of the partners and the EC is acknowledged. The authors wish to thank Pilar Pena, Angel Caballero and Antonio de Aza their help in the discussion of the equilibrium phase diagrams.

References

1. Spriet, P. and Habarou, G., Applications of CMCs to turbojet engines: overview of the SEP experience. *Key Eng. Mat.*, 1997, **127–131**, 1267–1276.
2. Vogel, W. D. and Spelz, U., Cost effective production techniques for continuous fiber reinforced ceramic matrix composites. In *Ceramic Processing Science and Technology*, ed. H. Hausner, G. L. Messing and S. I. Hirano. Ceramic Transactions, vol. 51, The American Ceramic Society, Westerville, OH, 1995. pp. 255–259.
3. Goujard, S., Vandenbulcke, L. and Tawil, H., The oxidation Y_2O_3 behaviour of two- and three-dimensional C/SiC thermostructural materials protected by chemical-vapour-deposition polylayers coatings. *J. Mat. Sci.*, 1994, **29**, 6212–6220.
4. Cavalier, J. C. and Nale, A., Procede pour la protection antioxydation de produits en materiau composite contenant du carbone, et produits obtenus par le procede. European Patent 0375537-A1, 19 December 1989.
5. Ogura, Y., Kondo, M. and Morimoto, T., Y_2SiO_5 as oxidation resistant coating for C/C composites. In Proceedings of the Tenth International Conference on Composite Materials, Vol. IV. Whistler, BC, Canada, 14–18 August, ed. A. Poursartip and K. Street. Woodhead Publishing Limited, 1995, pp. 767–774.
6. Webster, J. D., Westwood, M. E., Hayes, F. H., Day, R. J., Taylor, R., Durán, A., Aparicio, M., Rebstock, K. and Vogel, W. D., Oxidation protection coatings for C/SiC based on Y_2SiO_5. *Key Eng. Mat.*, 1997, **132–136**, 1641–1644.
7. Moreno, R., Moya, J. S. and Requena, J., Electroquímica de Suspensiones Cerámicas. *Bol. Soc. Esp. Ceram. Vidr.*, 1987, **26**, 355–365.
8. Yasrebi, M., Ziomek-Moroz, M., Kemp, W. and Sturgis, D. H., Role of particle dissolution in the stability of binary yttria–silica colloidal suspensions. *J. Am. Ceram. Soc.*, 1996, **79**(5), 1223–1227.
9. Yasrebi, M., Springgate, M. E., Nikolas, D. G., Kemp, W., Sturgis, D. H. and McCarthy, J. M., Colloidal stability of zirconia-doped yttria–silica binary aqueous Suspensions. *J. Am. Ceram. Soc.*, 1997, **80**(6), 1615–1618.
10. Levin, E. M., Robbins, C. R. and Mc Murdie, H. F., In *Phase Diagrams for Ceramists 1969 Supplement*. (Figures 2067–4149). Metal oxide systems. ed. M. K. Reser. The American Ceramic Society, Columbus, OH, 1969. pp.76–195.
11. Moreno, R., Salomoni, A. and Castanho, S. M., Colloidal filtration of silicon nitride aqueous slips. Part I. *J. Eur. Ceram. Soc.*, 1998, **18**, 405–416.